

Research Journal of Pharmaceutical, Biological and Chemical Sciences

Adsorption of melanoidin using microporous ZnO nano particle: Experimental and ANN approach.

Charles David^{1*} and M Arivazhagan².

¹Department of Biotechnology, VIGNAN's Foundation for Science, Technology and Research University, Vadlamudi, Guntur – 522 213, Andhra Pradesh, India

²Department of Chemical Engineering, National Institute of Technology, Tiruchirappalli – 620 015, Tamil Nadu, India

ABSTRACT

Degradation of highly recalcitrant pollutants present in the distillery effluent has gained considerable interests in surface water pollution control. This study deals with examining the efficiency of ZnO nanoparticles as adsorbents for decolorization of synthetic melanoidin. The batch adsorption experiments were conducted with varying range of three key process parameters *viz.*, adsorbent dosage, pH, and temperature with an objective to achieve maximum colour removal. The morphological and chemical characteristics of the nanoparticle were analyzed by X-ray diffraction spectroscopy, scanning electron microscopy, energy dispersive X-ray analysis, Brunauer–Emmett–Teller surface area analysis and Barrett–Joyner–Halenda pore size distribution analysis. A maximum of 90% decolorization of melanoidin was achieved with a dosage of 2.5 g/L, pH 3 at 30 °C. Using Artificial Neural Network (ANN), a two-layered feed-forward back propagation model contributed the most estimable performance as a predictive model for melanoidin decolorization.

Keywords: Melanoidin decolorization, nano-ZnO, adsorption, microporous, ANN

**Corresponding author*

Email: arcda88@gmail.com

INTRODUCTION

Distillery effluent contains prominent levels of fractious pollutants in the form of colour and organic compounds. The acute colour is due to the presence of a dark brown, acidic, colour pigment melanoidin [1]. Melanoidin is a nitrogenous polymer, generated as a product of Maillard reaction [2], a non-enzymatic reaction between carbohydrates and amino compounds [3, 4]. The chemical formula of melanoidin is $C_{17-18}H_{26-27}O_{10}N$ [5]. These recalcitrant polymers cannot be easily degraded by a general biological treatment process, namely, anaerobic lagoons, bio-methanation and aerated sludge processes [6,7]. Due to the antioxidant property of melanoidin, the microbial growth gets inhibited, which hinders the degradation of colour and toxicity [8]. Even though the spent wash does not contain any highly toxic pollutants, the intense colour of melanoidin pigments present in the untreated effluent, when released into the surface water resources, obstructs the sunlight penetration into the water, thereby decreases the photosynthetic activity and polluting the aquatic ecosystem [9]. Moreover, the effluent also contains high concentrations of biological oxygen demand (BOD), chemical oxygen demand (COD), total dissolved solids (TSS), acidic and an obnoxious odor. Therefore, a potential alternative for the degradation melanoidin pigment present in the effluent is a problem of major concern [10].

Physical-chemical treatment methods involve coagulation and flocculation, adsorption, electro-coagulation, advanced oxidation, ozonation, membrane filtration and evaporation. Adsorption is one of the major physical-chemical treatment methods employed for removing pollutants and colour. Regardless of the adsorbents employed, the decolorization process will be majorly influenced by factors namely, the initial concentration of the effluent, molecular size, charge density and concentration of the other pollutants that are present in the effluent. It is suggested that more surface area on the adsorbent enhances adsorption by enabling the adsorbate to get access to numerous micropores with high energy for adsorbing pollutant molecules [11].

The aim of this work was to inquire the treatment of synthetic melanoidin using microporous ZnO nanoparticles as an adsorbent. Experiments were carried out to learn the contributions of process parameters such as adsorbent dosage, pH, and the temperature in the batch adsorption process of melanoidin. The experimental data were trained, validated and predicted using Artificial Neural Network (ANN) tool in MATLAB to check the goodness of the experiment. Using the curve fitting tool, surface plots are drawn to identify the effect of mutual interaction between the key operating parameters. For the first time, pure ZnO nanoparticle was investigated for its ability towards decolorization of synthetic melanoidin and the experimental results were trained and validated using ANN method.

MATERIALS AND METHODS

ZnO Nanoparticle

Zinc oxide (ZnO), 99% pure, with a particle size 20–30 nm and surface area of 60–65 m²/g was procured from Sisco Research Laboratories (SRL) Pvt. Ltd., India. To remove the moisture content, the stock ZnO nanoparticles were calcined in a box furnace at 200 °C for 120 min.

Characterization of ZnO nanoparticle

XRD patterns were read using a Rigaku, Ultima IV, powder X-ray diffractometer with Cu α radiation ($\lambda = 0.15406$ nm), the 2θ range of 20° – 80° and with continuous scanning type at a scanning speed of 2°/min to evaluate the crystalline property of the sample. The surface morphology of the pure ZnO was analysed using Hitachi, Model S4800 Scanning Electron Microscope (SEM). Energy-dispersive X-ray spectroscopy (EDX) to evaluate the purity of the sample in terms of elemental compositions was conducted using the Horiba EDX instrument equipped with the SEM. The surface area of the sample was determined by Brunauer–Emmett–Teller (BET) method and the pore size distribution was determined by Barrett–Joyner–Halenda (BJH) plot. The sample tube containing the sample was weighed before regeneration. The sample was pre-heated in the presence of nitrogen using Belprep Vac II. The samples were regenerated at 250°C for two hours in the presence of the vacuum (10^{-2} kPa). The difference in the weight of the sample before and after regeneration under vacuum gives the sample quantity. The surface area and porosity of the adsorbents were analyzed using volumetric gas adsorption methods using Belsorp Mini II. The sample cell containing the regenerated sample

was loaded to Belsorp Mini II and the adsorption and desorption onto the sample occurs and the surface area and the pore size distribution can be evaluated.

Experimental procedure

Melanoidin was prepared synthetically by mixing 4.5 g of glucose, 1.88 g of glycine and 0.42 g of sodium bicarbonate (Merck) with 100 mL of distilled water and heating at 95 °C for 7 h [12]. To the dark brown slurry that is formed, 100 mL of distilled water was added to prepare a melanoidin stock solution. The prepared solution had a COD concentration of 29,500 mg/L. The necessary dilutions of stock melanoidin solutions were prepared as sorbate for colour removal studies.

A five-level-three-factor experimental design consisting 125 experiments were performed considering the three independent variables viz. the adsorbent (ZnO) dosage, pH, and temperature. Percentage colour removal was considered as the experimental output response. The process parameters of the experiment were operated between the range of 0.5–2.5 g/L for adsorbent dosage, pH 3–11, and temperature 25–45 °C respectively.

The batch adsorption process was performed in Erlenmeyer flasks (250 mL volume) containing 100 mL of synthetic melanoidin solution. An appropriate dosage of ZnO nanoparticle was added and the pH of the solution was adjusted using dilute NaOH and HCl. The batch vessels were shifted to an incubator shaker and the suspension was shaken at 200 rpm to suspend the adsorbent particles in the solution. After 180 minutes, aliquots of samples were withdrawn and centrifuged at 10000 rpm to remove the suspended particles. Colour removal was quantified at a wavelength of 475 nm using UV-Visible spectrophotometer. The baseline calibration to the spectrophotometer was done using distilled water as blank sample.

The colour removal efficiency was calculated by:

$$\text{Colour removed (\%)} = \frac{C_0 - C_t}{C_0} \times 100 \quad (1)$$

where, C_0 and C_t are the initial absorbance and absorbance at the time t for the synthetic melanoidin solution at a characteristic wavelength of 475 nm [13, 14, 15].

Artificial Neural Network method

ANNs behaves as a “black box” model, which consists of interconnected processing units known as neurons or nodes [16]. This computational tool has been widely employed as an alternative methodology in different areas, such as problems of prediction, classification, modelling, simulation or control [17, 18]. Out of many types of ANNs developed, the feed-forward back propagation neural network is a popular method which consists of an input layer, one or more hidden layers, and an output layer. The performance of the neural network depends on the number of hidden layers and the number of neurons in the hidden layers. By altering the number of hidden layers as well as the number of neurons in the hidden layers through trial and error method, a suitable neural network architecture was selected. In our study, the final architecture of the ANN model was 3–10–10–1 (3 neurons in the input layer, 10 neurons in the first hidden layer, 10 neurons in the second hidden layer and 1 neuron in the output layer) was considered and shown in Fig. 1. The nodes between each layer relate to adaptable weights. While training the network, the weights must be adjusted to minimize the differences between the output of the network and the experimental results. The training parameters are listed in the Table 1.

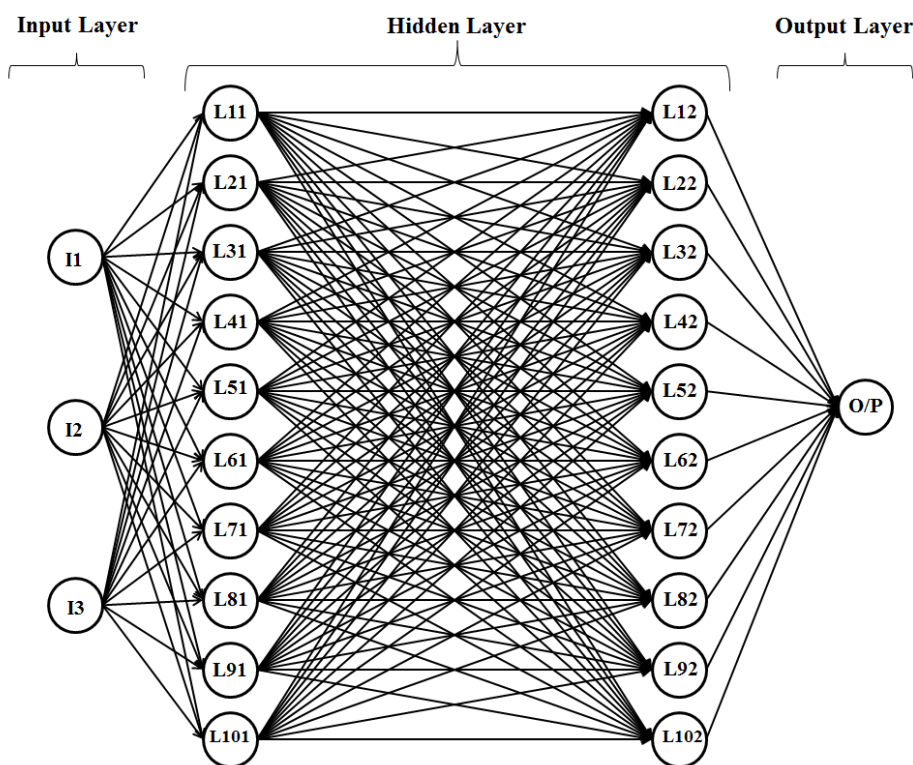


Figure 1: Architecture of Artificial Neural Network (ANN)

Table 1: Parameters considered for training the ANN model

Training parameters	Value
Training algorithm	Levenberg–Marquardt (LM) algorithm
Performance function	Mean Squared Error (MSE)
Input layer activation function	Nil
Hidden layer activation function	'tansig'
Output layer activation function	'purelin'
Number of Input layer nodes	3
Number of Hidden layers	2
Number of nodes per Hidden layer	10
Number of Output layer nodes	1
Generalization method	Early stopping

The mean squared error (MSE) is usually used as the performance function to interpret the difference between the output of ANN and the actual value. The experimental data is fed into the ANN tool and trained with Feed-forward back propagation, mean squared error (MSE) method. The number of the neurons in input and output layer was determined with respect to the number of experimental input variables and output response. The three process parameters such as catalyst dosage, pH, and temperature were considered as the input variables and the experimental response in terms of percentage colour removed was considered as the output variable.

A combination of 'tansig' and 'purelin' functions were used as the activation functions for the hidden layer and output layer. The ANN summary of this study is shown in Fig. 2. The Levenberg–Marquardt (LM) algorithm which is one of the most widely used algorithms with more accuracy was chosen as the training algorithm. All other ANN parameters were set as default values as in the ANN tool in MATLAB. The network was trained for 1000 epoch.

During the training process, a common problem of over-fitting occurs which can be solved by early stopping. To perform an early stopping method, the available data must be divided into three data sets, such as training set, validation set, and the test set. Among these, only the training set is used for training the network. Once the validation error increases with a decrease in training error, it indicates that ANN starts to over-fit. The continuous increase in the validation error for a preset number of iterations results in termination of the training process. The test set data will be considered as hidden data for final testing of the trained ANN. Early stopping results in better results. In this study, the experimental results of 125 data were split randomly into three data sets, 70% of the training set, 15% of the validation set and 15% of the test set.



Figure 2: Summary of the ANN model.

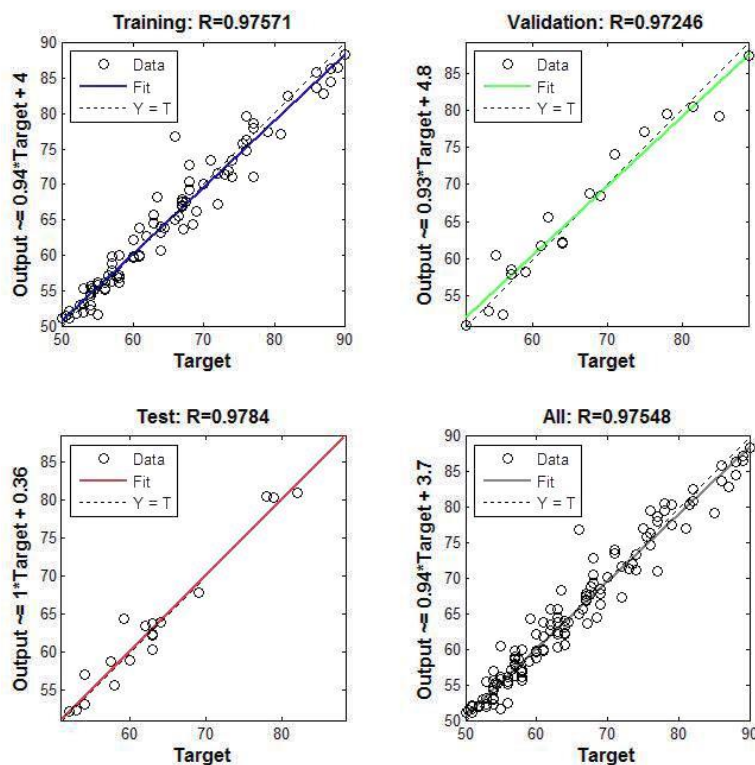


Figure 3: Parity plots of predicted values versus experimental values.

When the iteration reaches the minimal gradient value, the performance validation and the regression were tested. It has been observed from the performance plot that the values of train data, validation data, and test data almost converge with the best fit line. It is also concluded that the experiments, as well as the theoretical trials comparatively, have the minimal error correspondingly, the gradient reaches a minimum of 0.01 at epoch 17. From the regression analysis plots, the validation and test result in terms of error were dealt. From Fig. 3, it has been noted that the fit data and the experimental data almost coincides with each other with an R value of 0.97571, 0.97246 and 0.9784 for training, validation and test data sets respectively.

Since the R value approaches almost 97% it can be interpreted that the experimental error is minimum and experimental data and model predictions are in excellent agreement. By using the curve fitting tool in MATLAB, the mutual interactions between the key operating parameters were identified by plotting surface plots.

RESULTS AND DISCUSSION

Characterization of ZnO nanoparticle

The crystal characterization of ZnO nanoparticle was shown in Fig. 4(a). The highly crystalline characteristics of the ZnO nanoparticle were elucidated with the occurrence of sharp and intense peaks. From the XRD profile of ZnO, the signature peaks belonging to pure zinc oxide with high intensity of reflections at angles (2θ) around 31° , 35° , 37° , 48° , 56° , 62° , 68° , and 69° can be noticed. The peaks at afore mentioned angles correspond to the reflection from (100), (002), (101), (102), (110), (103), (200) and (112) crystal planes respectively [19]. The X-ray diffraction pattern can be used to identify the crystal phase and to estimate the crystal size at each phase. The XRD diffraction pattern reveals the presence of a single hexagonal phase with Wurtzite structure (JCPDS No. 36-1451) and with lattice constants $a=b=3.2492 \text{ \AA}$ and $c=5.20661 \text{ \AA}$. SEM image of ZnO nanoparticles was captured at 150,000 magnifications shown in Fig. 4 (b). From the SEM micrograph of ZnO, vaguely hexagonal-shaped nanoparticles with an average particle size of 23 nm with a high extent of agglomeration can be visualized. The Energy Dispersive X-ray (EDX) spectrum for composition analysis is shown in Fig. 4 (c).

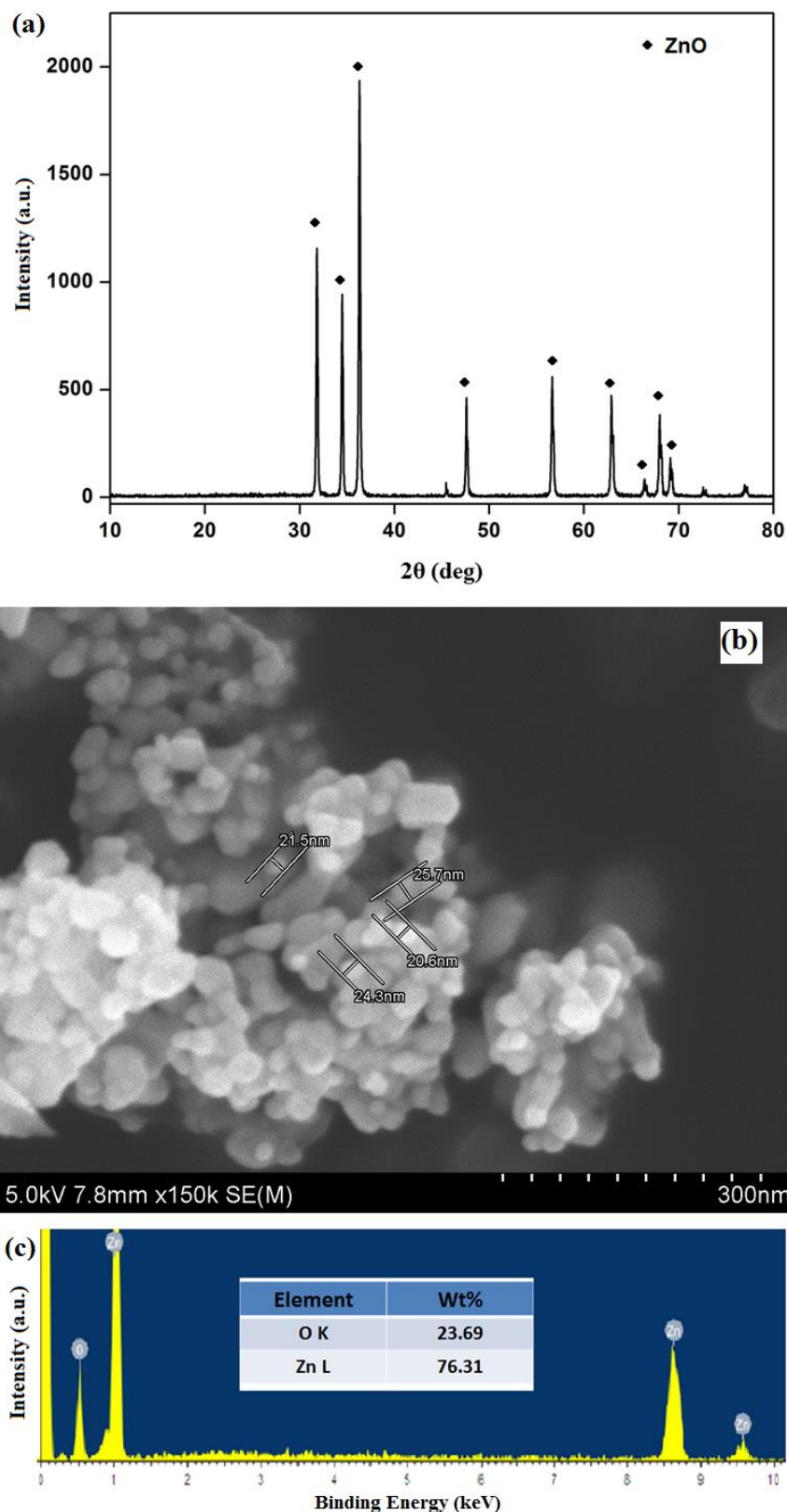


Figure 4: (a) XRD diffractogram, (b) SEM micrograph and (c) The EDX spectrum of ZnO.

BET surface area and BJH pore size distribution analysis

The N₂ adsorption/desorption isotherm and the pore size distribution curve for microporous ZnO nano-adsorbents is shown in Fig. 5. Approximately 250 mg of the ZnO nano powder was taken in the sample

cell and degassed at 250 °C for 180 min under vacuum degassing condition. Degassing of the sample facilitates the removal of moisture and adsorbed gases from the sample. The sample was then subjected to adsorption by admitting a known quantity of nitrogen gas to the sample cell maintained at a constant temperature of -196°C using liquid nitrogen. Adsorption occurs and due to the adsorption of nitrogen gas by the sample, a change in pressure occurs in the sample cell. The pressure difference data were recorded until it reaches the equilibrium. BET plot (adsorption/desorption isotherm) was drawn between relative pressure (p/p^0) versus volume of N₂ gas adsorbed (cm³/g) and the surface area was calculated to be 63.66 m²/g of ZnO nanoparticles. The BJH plot (pore size distribution) for microporous ZnO is shown in Fig. 5 (inset). The pure ZnO sample had a pore diameter of 15 Å.

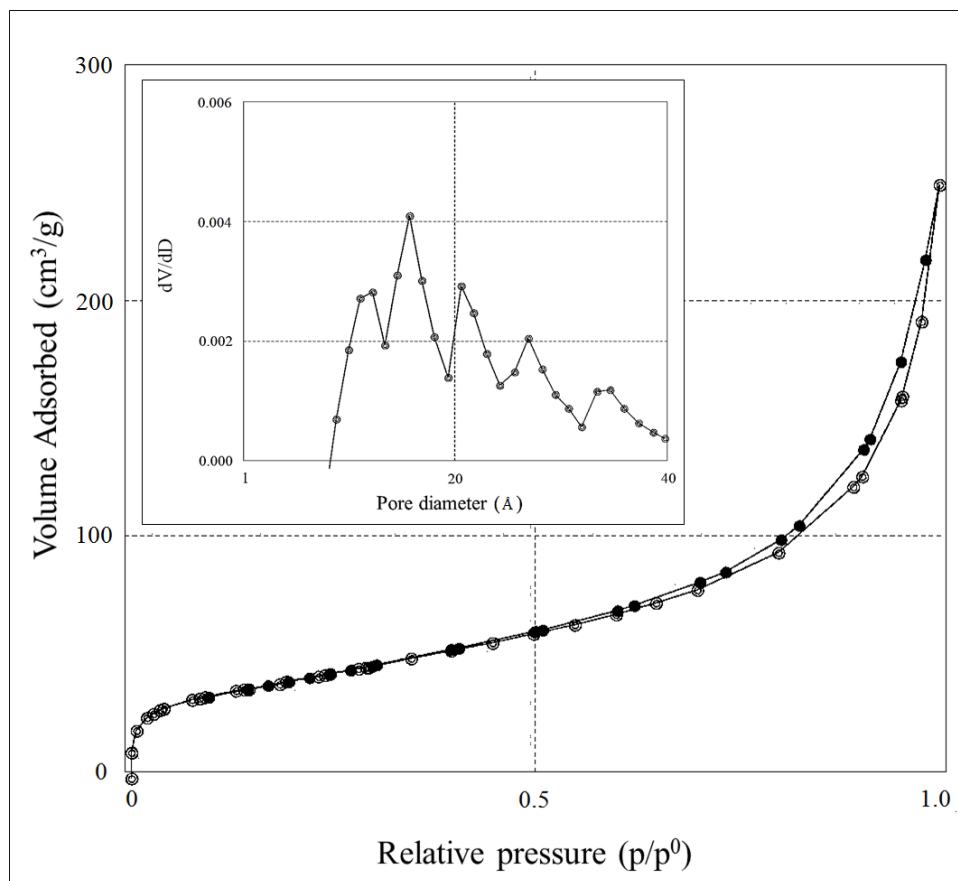


Figure 5: BET plot (adsorption / desorption isotherm), Inset:BJH plot (pore sizedistribution) for ZnO.

ANN analysis

In this study, 125 experimental input data and results were used to develop and validate the ANN method. It is found that consideration of the interactions between the process parameters. However, the ANN method could learn to account for the adsorption process and the interactions between the process parameters to some extent during the training process and save it in the “black box” model, thereby resulting in the better prediction of the experimental results. A Feed-forward back propagation model was developed with dimensionless input variables such as adsorbent dosage, pH, and temperature. The experimental output was in terms of colour removal efficiency. The experimental input data were validated and tested for the best fit using the ANN tool. The ANN architecture of 3–10–10–1 (3 neurons in the input layer, 10 neurons, each for two hidden layers and 1 neuron in the output layer) was considered and the convergence took place at the 17th iteration. The performance of the adsorption process was evaluated using the neural network and validated graphically. The gradient measures 4.7181 and correspondingly, the ‘mu’ reaches a minimum at epoch 17.

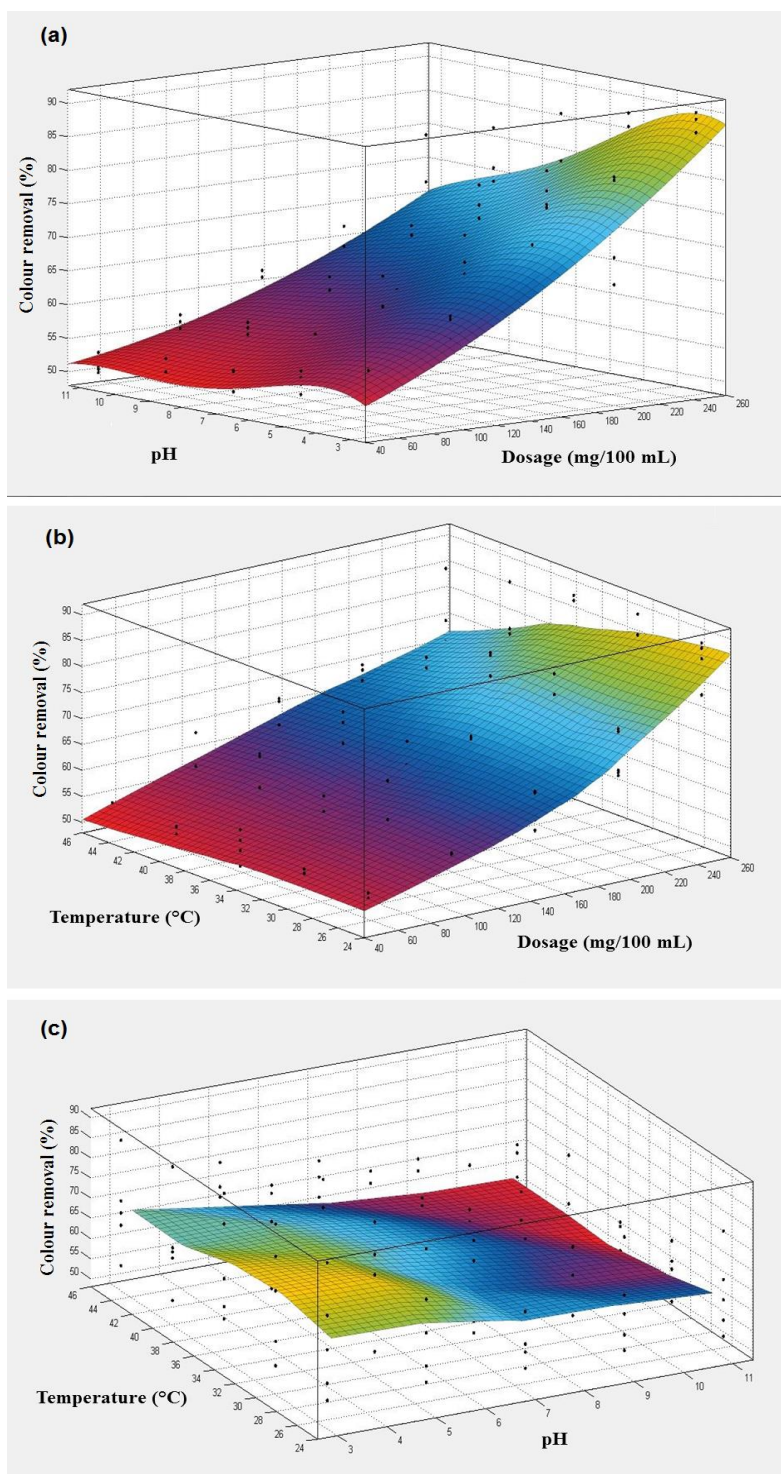


Figure 6: Surface plots showing interactions between process parameters: (a) dosage, pH vs. % colour removal, (b) dosage, temperature vs. % colour removal, (c) pH, temperature vs. % colour removal.

The Effect of process parameters on adsorption efficiency

The mutual interaction between the operating parameters in terms of percentage colour removed was plotted using the curve fitting tool in MATLAB. Surface plots showing interactions between the adsorbent dosage, pH vs. % colour removed, adsorbent dosage, temperature vs. % colour removed and pH, temperature vs. % colour removed are shown in Fig. 6 (a), (b) and (c). From the surface plots, it was clear that the ZnO dosage has much impact on the colour removal efficiency followed by pH and temperature. Adsorption

efficiency was high under acidic conditions and higher adsorbent dosage levels as shown in Fig. 6 (a). At the lower temperature range of 25–35 °C, even moderate adsorbent dosage concentrations resulted in better colour removal efficiency. However, at higher adsorbent dosage concentrations, decolorization efficiency was high. There was not as much influence on the colour removal efficiency due to the mutual interaction between pH and temperature as shown in Fig 6 (c). The Root Mean Squared Error (RMSE) and correlation coefficients R-square is calculated and the results are reported in the Table 2. From the results, it can be elucidated that, the mutual interaction between dosage and pH had much of an effect on the adsorption efficiency of the ZnO nanoparticles with a higher R-square value of 0.8997 and a lowest RMSE value of 3.4604. The interaction between pH and temperature on the colour removal efficiency was minimal with an R-square value of 0.1757.

Table 2: Effect of mutual interactions between the process parameters

Interactions	R-square	RMSE
Dosage, pH vs. % colour removed	0.8997	3.4604
Dosage, Temperature vs. % colour removed	0.7655	5.2406
pH, Temperature vs. % colour removed	0.1757	---

The linear polynomial equation for the effect of the adsorbent dosage and pH on colour removal efficiency was given as follows:

$$f(x,y) = p00 + p10*x + p01*y + p20*x^2 + p11*x*y + p02*y^2 + p21*x^2*y + p12*x*y^2 + p03*y^3 + p22*x^2*y^2 + p13*x*y^3 + p04*y^4;$$

Coefficients (with 95% confidence level) are as follows:

p00 = 63.16 (61.38, 64.95);	p10 = 9.046 (8.086, 10.01);
p01 = -5.242 (-7.232, -3.251);	p20 = 1.092 (-0.05911, 2.244);
p11 = -1.997 (-3.854, -0.1397);	p02 = 2.011 (-2.41, 6.431);
p21 = -0.0822 (-0.824, 0.6596);	p12 = -0.1632 (-0.905, 0.5786);
p03 = 0.896 (-0.1383, 1.93);	p22 = 0.06263 (-0.8275, 0.9528);
p13 = 0.1362 (-0.9024, 1.175);	p04 = -0.9112 (-2.854, 1.032).

CONCLUSION

In this paper, microporous ZnO nanoparticles have been synthesized and characterized using XRD, SEM, EDX, BET surface area analysis and BJH pore size distribution analysis. Batch adsorption experiments were conducted to determine the optimized process parameters for melanoidin adsorption. An adsorbent dosage of 2.5 g/L, pH 3 and at 30 °C resulted in 90% decolorization of the synthetic melanoidin solution. 125 experimental data and results were trained and regression analysis was performed using ANN which presented the best accuracy with an overall correlation coefficient of 0.97548. Using the polynomial curve fitting tool, surface plots have been plotted to visualize the mutual interaction between the key process variables namely, the adsorbent dosage, pH, and temperature. The surface plots reflect that the interactions between adsorbent dosage, pH and the interactions between adsorbent dosage, the temperature had much effect on adsorption of melanoidin pigments onto microporous ZnO nanoparticles.

ACKNOWLEDGEMENTS

The authors would like to extend their gratitude towards the SEM and EDX Facility (Funded by DST – India), Chemical Engineering Department, IIT Madras, Chennai. The authors also thank Dr. Shobin L.R, Centre for Nano and Soft Matter Sciences, Bangalore, for his valuable suggestions.

Declaration of interest: The authors report no declarations of interest.



REFERENCES

- [1] Bernardo EC, Egashira R, Kawasaki J. Carbon 1997; 35, 1217–1221.
- [2] Wedzicha BL, Kaputo MT. Food Chemistry 1992; 43, 359–367.
- [3] Migo VP, Matsumara M, Rosario EJD, Kataoka H. 1993. J of Fermentation and Bioengineering 1993; 75, 438–442.
- [4] Naik N, Jagadeesh KS, Noolvi MV. Iranian J of Energy Environment 2010; 1, 347–351.
- [5] Manisankar P, Rani C, Viswanathan S. Chemosphere 2004; 57, 961–966.
- [6] Satyawali Y, Balakrishnan M. Bioresource Technology 2007; 98, 2629–2635.
- [7] Zhou Y, Liang Z, Wand Y. Desalination 2008; 55, 301–311.
- [8] Pant D, Adholeya A. Bioresource Technology 2007; 98, 2321–2334.
- [9] Prasad RK. J of Hazardous Materials 2009; 165, 804–811.
- [10] Kalavathi DF, Uma L, Subramanian, G. Enzyme and Microbial Technology 2001; 29, 246–251.
- [11] Figaro S, Louisy-Louis S, Lambert J, Ehrhardt JJ, Ouensanga A, Gaspard S. Water Research 2006; 40, 3456–3466.
- [12] Bernardo EC, Egashira R., Kawasaki J. Carbon 1997; 35, 1217–1221.
- [13] David C, Narlawar R, Arivazhagan M. 2015. J of Indian Chemical Engineer 2016; 58, 198–200.
- [14] Raghukumar C, Rivonkar G. Applied Microbiology and Biotechnology 2001; 55, 510–514.
- [15] Prasad RK, Srivastava SN. J of Hazardous Materials 2009; 161, 1313–1322.
- [16] Kalogirou SA. Renewable and Sustainable Energy Reviews 2001; 5, 373–401.
- [17] Nagesh DS, Datta GL. J of Materials Processing Technology 2002; 123, 303–312.
- [18] Mohanty YK, Mohanty BP, Roy GK, Biswal KC. Chemical Engineering J2009; 148, 41–49.
- [19] Gu F, Wang SF, Lu MK, Zhou GJ, Xu D, Yuan, DR. Langmuir 2004; 20, 3528–3531.